Three types of couplings between asymmetric plasmonic dimers

Yen-Chun Chao,[1] Hsuan-Chi Tseng,[1,2] Kao-Der Chang,[3] and Chih-Wei Chang[1,*]

[1]*Center for Condensed Matter Sciences, National Taiwan University, Taipei 10617, Taiwan*
[2]*Department of Electro-Optical Engineering, National Taipei University of Technology, Taipei 10608, Taiwan*
[3]*Nanotechnology Research Center, Industrial Technology Research Institute, Hsinchu 31040, Taiwan*
[*]*cwchang137@ntu.edu.tw*

Abstract: We report extensive numerical studies on plasmonic dimers of different configurations and find that their coupling effects can be categorized into three types of phenomena. First, like ordinary mechanical systems, the plasmonic dimers can exhibit positive couplings that show anti-crossing behavior. Second, they can also be arranged to exhibit negative couplings that display opposite trends in resonant frequency shifts. Third, when there are surface currents in proximity to each other, the resonance frequencies of the dimers exhibit unusual redshifts that do not have any analogies in conventional systems. Our work suggests that in addition to the well-known electric and magnetic dipolar interactions, contributions from the inductance of displacement currents in the near field cannot be ignored. Overall, asymmetric plasmonic dimers exhibit better sensitivities than the symmetric counterparts and our extensive studies also enable us to identify the plasmonic dimer with the highest sensing capabilities.

OCIS codes: (250.5403) Plasmonics; (310.6628) Subwavelength structures, nanostructures.

References and links

1. J. N. Anker, W. P. Hall, O. Lyandres, N. C. Shah, J. Zhao, and R. P. Van Duyne, "Biosensing with plasmonic nanosensors," Nat. Mater. **7**(6), 442–453 (2008).
2. M. E. Stewart, C. R. Anderton, L. B. Thompson, J. Maria, S. K. Gray, J. A. Rogers, and R. G. Nuzzo, "Nanostructured plasmonic sensors," Chem. Rev. **108**(2), 494–521 (2008).
3. V. M. Shalaev, "Optical negative-index metamaterials," Nat. Photonics **1**(1), 41–48 (2007).
4. N. I. Zheludev, "Applied physics. The road ahead for metamaterials," Science **328**(5978), 582–583 (2010).
5. S. Zhang, D. A. Genov, Y. Wang, M. Liu, and X. Zhang, "Plasmon-induced transparency in metamaterials," Phys. Rev. Lett. **101**(4), 047401 (2008).
6. N. Liu, H. Liu, S. Zhu, and H. Giessen, "Stereometamaterials," Nat. Photonics **3**(3), 157–162 (2009).
7. T. Kaelberer, V. A. Fedotov, N. Papasimakis, D. P. Tsai, and N. I. Zheludev, "Toroidal dipolar response in a metamaterial," Science **330**(6010), 1510–1512 (2010).
8. C. Menzel, C. Helgert, C. Rockstuhl, E. B. Kley, A. Tünnermann, T. Pertsch, and F. Lederer, "Asymmetric transmission of linearly polarized light at optical metamaterials," Phys. Rev. Lett. **104**(25), 253902 (2010).
9. C. W. Chang, M. Liu, S. Nam, S. Zhang, Y. Liu, G. Bartal, and X. Zhang, "Optical Möbius symmetry in metamaterials," Phys. Rev. Lett. **105**(23), 235501 (2010).
10. K. H. Su, Q. H. Wei, X. Zhang, J. J. Mock, D. R. Smith, and S. Schultz, "Interparticle coupling effects on plasmon resonances of nanogold particles," Nano Lett. **3**(8), 1087–1090 (2003).
11. B. M. Reinhard, M. Siu, H. Agarwal, A. P. Alivisatos, and J. Liphardt, "Calibration of dynamic molecular rulers based on plasmon coupling between gold nanoparticles," Nano Lett. **5**(11), 2246–2252 (2005).
12. P. K. Jain, S. Eustis, and M. A. El-Sayed, "Plasmon coupling in nanorod assemblies: optical absorption, discrete dipole approximation simulation, and exciton-coupling model," J. Phys. Chem. B **110**(37), 18243–18253 (2006).
13. O. L. Muskens, V. Giannini, J. A. Sánchez-Gil, and J. Gómez Rivas, "Optical scattering resonances of single and coupled dimer plasmonic nanoantennas," Opt. Express **15**(26), 17736–17746 (2007).
14. P. K. Jain and M. A. El-Sayed, "Noble metal nanoparticle pairs: effect of medium for enhanced nanosensing," Nano Lett. **8**(12), 4347–4352 (2008).
15. A. M. Funston, C. Novo, T. J. Davis, and P. Mulvaney, "Plasmon coupling of gold nanorods at short distances and in different geometries," Nano Lett. **9**(4), 1651–1658 (2009).
16. P. K. Jain and M. A. El-Sayed, "Plasmonic coupling in noble metal nanostructures," Chem. Phys. Lett. **487**(4-6), 153–164 (2010).

#157877 - $15.00 USD Received 8 Nov 2011; revised 28 Dec 2011; accepted 3 Jan 2012; published 24 Jan 2012

17. P. K. Jain, W. Y. Huang, and M. A. El-Sayed, "On the universal scaling behavior of the distance decay of plasmon coupling in metal nanoparticle pairs: A plasmon ruler equation," Nano Lett. **7**(7), 2080–2088 (2007).
18. S. Sheikholeslami, Y. W. Jun, P. K. Jain, and A. P. Alivisatos, "Coupling of optical resonances in a compositionally asymmetric plasmonic nanoparticle dimer," Nano Lett. **10**(7), 2655–2660 (2010).
19. F. J. García de Abajo, "Nonlocal Effects in the Plasmons of Strongly Interacting Nanoparticles, Dimers, and Waveguides," J. Phys. Chem. C **112**(46), 17983–17987 (2008).
20. C. Tabor, R. Murali, M. Mahmoud, and M. A. El-Sayed, "On the use of plasmonic nanoparticle pairs as a plasmon ruler: the dependence of the near-field dipole plasmon coupling on nanoparticle size and shape," J. Phys. Chem. A **113**(10), 1946–1953 (2009).
21. T. Li, R. X. Ye, C. Li, H. Liu, S. M. Wang, J. X. Cao, S. N. Zhu, and X. Zhang, "Structural-configurated magnetic plasmon bands in connected ring chains," Opt. Express **17**(14), 11486–11494 (2009).
22. H. Liu, D. A. Genov, D. M. Wu, Y. M. Liu, J. M. Steele, C. Sun, S. N. Zhu, and X. Zhang, "Magnetic plasmon propagation along a chain of connected subwavelength resonators at infrared frequencies," Phys. Rev. Lett. **97**(24), 243902 (2006).
23. D. F. Bartlett and T. R. Corle, "Measuring Maxwell's displacement current inside a capacitor," Phys. Rev. Lett. **55**(1), 59–62 (1985).
24. D. F. Bartlett and G. Gengel, "Measurement of quasistatic Maxwell's displacement current," Phys. Rev. A **39**(3), 938–945 (1989).
25. S. M. Godin and V. V. Botvinovskii, "Measurement of displacement currents by a fammeter," J. Commun. Technol. Electron. **54**(9), 1092–1095 (2009).
26. P. Nordlander, C. Oubre, E. Prodan, K. Li, and M. I. Stockman, "Plasmon hybridizaton in nanoparticle dimers," Nano Lett. **4**(5), 899–903 (2004).
27. L. V. Brown, H. Sobhani, J. B. Lassiter, P. Nordlander, and N. J. Halas, "Heterodimers: plasmonic properties of mismatched nanoparticle pairs," ACS Nano **4**(2), 819–832 (2010).
28. E. R. Encina and E. A. Coronado, "On the Far Field Optical Properties of Ag-Au Nanosphere Pairs," J. Phys. Chem. C **114**(39), 16278–16284 (2010).
29. O. Arcizet, P. F. Cohadon, T. Briant, M. Pinard, A. Heidmann, J. M. Mackowski, C. Michel, L. Pinard, O. Français, and L. Rousseau, "High-sensitivity optical monitoring of a micromechanical resonator with a quantum-limited optomechanical sensor," Phys. Rev. Lett. **97**(13), 133601 (2006).

1. Introduction

Prior to the advent of quantum mechanics, chemists had extensively studied the solubility of various kinds of matters and categorized them into different groups. The knowledge acquired during the period later became the basis of chemical bonds. The significance of these works should now apply to understanding artificial atoms and molecules exhibiting plasmonic resonances. These artificial nanoscale metal structures exhibit strong electric or magnetic responses at optical frequencies and have been widely utilized for exploring new optical phenomena [1,2]. In these plasmonic systems, a basic element such as a metal rod or a split-ring resonator can be considered as an artificial atom (i.e. meta-atom). Because the optical responses of these meta-atoms can be tailored by engineering their subwavelength geometries, they open many degrees of freedom for designing optical elements with properties going far beyond those of conventional materials [3]. Various extraordinary phenomena such as negative refraction, reversal of phase/group velocity, optical information storage, optical tunneling and optical cloaking can now be realized using meta-atoms with designed functionalities [4].

When two or more meta-atoms are assembled into artificial molecules (i.e. metamolecules), additional degrees of freedom are added to their designs. Even though the underlying mechanisms are within the classical domain of electrodynamics, many interesting phenomena that go beyond conventional chemical bonds can be found. For example, coupling two meta-atoms can result in phenomena mimicking electromagnetically induced transparency, asymmetric transmission, stereometamaterial or toroidal dipolar responses [5–8]. Moreover, when three or six meta-atoms are assembled into trimers or hexamers, great engineering flexibilities in their designs allow metamolecules to realize a previously unfound new symmetry and topological effects [9]. From an application's point of view, dimers made of two nanoparticles have been widely utilized for detecting chemical or biological molecules [10–16]. Unfortunately, although the dimers represent the simplest form of metamolecules, the coupling between a dimer remains poorly understood [17]. Especially, if no structural symmetries can be found in a dimer, their optical responses yield unexpected phenomena [18]. Besides, it is worthy to know which dimer structures will exhibit the highest environmental sensitivities. Here we employ extensive numerical simulations to study

#157877 - $15.00 USD Received 8 Nov 2011; revised 28 Dec 2011; accepted 3 Jan 2012; published 24 Jan 2012

coupling behavior of dimers of various configurations. Our results show that despite the diverse geometrical or structural variations of plasmonic dimers, their interactions can be categorized into three kinds of coupling effects, which result from electric dipolar interactions, magnetic dipolar interactions, and a previously unfound effect arising from added inductance of near field displacement currents. The coupling effects, especially the negative couplings and the unusual redshifts, do not have any analogies in natural chemical bonds and thus metamolecules can exhibit richer optical phenomena than conventional materials.

2. Methods

We employed finite-difference-time-domain (FDTD) simulation methods using software package CST Microwave Studio to study the optical resonances of various plasmonic dimers with varying distances. Due to the broken structural symmetry, no optically-dark mode can be found in these asymmetric dimers. Thus all of the resonances can be identified from dips of transmission or peaks of reflection. To avoid non-local effects at small distances, we restricted the distance to be larger than 2nm [19]. The substrate is sapphire (refraction index = 1.7). The dimensions of the systems are always subwavelength ($<\lambda/4$) so that phase retardation effects can be neglected. The electrical conductivity of gold is described by the Drude model with plasmon frequency 1.37×10^{16} Hz and a practical damping rate 1.2×10^{14} Hz. To ensure simulation accuracy, the mesh size was kept less than $\lambda/2000$.

3. Results and discussions

Figure 1 summarizes our main findings from extensive numerical studies of more than 20 asymmetric metamolecular dimers. Despite the diverse geometrical variations one can design for an artificial dimer, our extensive works show that they can be reduced to a few representative dimers. In fact, as we will show later, the couplings of a dimer only concern how electric dipoles, magnetic dipoles, and surface currents are distributed. Thus only a few representative dimers are shown in Fig. 1 for clarity. Figure 1 shows that all the coupling phenomena of plasmonic dimers can be categorized into three types. The structural asymmetries make the resonance frequency of each meta-atom to be different and the conservation of degrees of freedom imposes the metamolecules to exhibit two resonances. Moreover, the structural asymmetry makes both resonances to be optically bright for a normal incidence light. Thus the two resonances can be identified from the dips of transmittance or from the peaks of reflectance. Note that the polarizations of the incident light can excite different modes of resonances. Thus different coupling behavior may occur when the incident polarization varies.

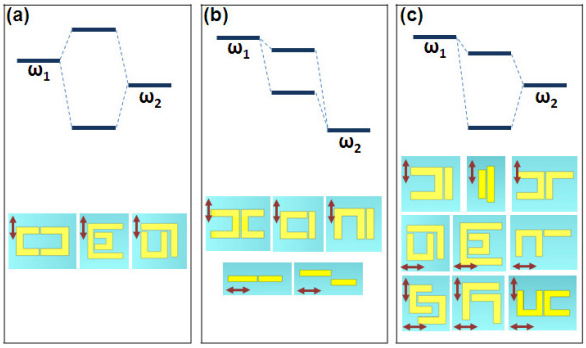

Fig. 1. Coupling diagrams of asymmetric metamolecules. Despite the diverse structural variations, our extensive numerical simulations reveal that there are only three types of couplings in metamolecules consisting of two meta-atoms. The coupling phenomena can be categorized into (a) type I (positive couplings), (b) type II (negative couplings), and (c) type III (two redshifts), respectively. The arrows denote the polarization of the normally incident light.

#157877 - $15.00 USD Received 8 Nov 2011; revised 28 Dec 2011; accepted 3 Jan 2012; published 24 Jan 2012

Figure 1(a) depicts an ordinary coupling effect (type I) and various dimers that belong to this category. In type I, the coupling effect is similar to coupled mechanical oscillators, i.e., the resulting resonances show anti-crossing behavior that one blueshift (antisymmetric mode) and one redshift (symmetric mode) are observed. Like mechanical systems, the result indicates that the effect can be described by a positive coupling constant between the meta-atoms.

In contrast to Fig. 1(a), type II coupling shown in Fig. 1(b) displays opposite frequency shifts that indicate a negative coupling constant. Both positive and negative couplings have been shown to exist in various metamolecules, and they originate from interactions of electric or magnetic dipoles of different orientations. Perhaps the most convincing proof of negative couplings is from a trimer metamolecule in which three negative couplings result in a degenerate resonance characteristically different from that of a positively-coupled trimer [9]. Negative couplings can also be identified from electromagnetic simulations in which the resonant frequency of the antisymmetric mode is lower than that of the symmetric mode.

Apart from the positive couplings and the negative couplings that always exhibit one blueshift and one redshift, we also discover a third type of couplings (type III) that the resonant frequency of a dimer show two redshifts respective to that of a meta-atom. As shown in Fig. 1(c), a large group of dimers displays the type III coupling effect. The two redshifts shown in Fig. 1(c) is very unusual and does not have any analogies in conventional systems. Moreover, unlike previous works that were limited to special plasmonic structures [20], we emphasize that our extensive studies demonstrate that type III coupling is very common in plasmonic dimers. Furthermore, unlike previous works that attributed the unusual couplings to some particular transitions of metals [18], our results suggest that the unusual coupling arises from a more universal electromagnetic phenomenon. In the following, we will show that type III coupling originates from added inductance of Maxwell's displacement currents.

We plot the resonance frequencies as a function of distance for type I, type II, and type III in Figs. 2(a), (b), (c), respectively. Three representative dimers from each category are chosen to display the coupling effect. Because couplings become stronger at short distances, increasing blueshifts and redshifts are clearly shown in Figs. 2(a) and (b) as the distance between meta-atoms decreases. Notably, the type I and type II display opposite trends as the distance decreases, which highlight the opposite signs of their coupling constants. Remarkably, Fig. 2(c) shows two redshifts as the distance decreases, an effect that is difficult to explain within conventional coupling theories.

To account for the observed coupling phenomena of various dimers, we here propose the following Lagrangian model for phenomenological understandings. We will discuss its

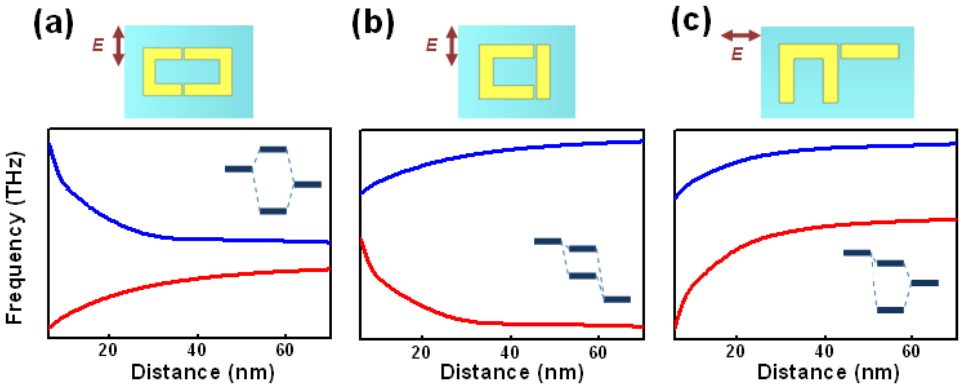

Fig. 2. Simulated resonant frequency shifts with respective to distances between two meta-atoms for three representative metamolecules in each type of couplings. The arrows denote the polarization of the normally incident light. The dashed lines are fitting results using solutions of Eq. (2).

#157877 - $15.00 USD Received 8 Nov 2011; revised 28 Dec 2011; accepted 3 Jan 2012; published 24 Jan 2012

electromagnetic foundations later. The Lagrange of a plasmonic dimer can be generally expressed as:

$$L = \frac{1}{2}L_1\dot{Q}_1^2 + \frac{1}{2}L_2\dot{Q}_2^2 - \frac{1}{2}L_1\omega_1^2Q_1^2 - \frac{1}{2}L_2\omega_2^2Q_2^2 - M_e\omega_1\omega_2Q_1Q_2 - M_m\dot{Q}_1\dot{Q}_2 + \frac{1}{2}L'(\dot{Q}_1 - \dot{Q}_2)^2 \qquad (1)$$

where L_1, L_2 are the inductance, Q_1, Q_2 are the charges, ω_1, ω_2 are resonance frequencies of individual meta-atom. M_e, M_m, and L' are respectively the magnetic coupling, the electric coupling, and the inductance from displacement currents (explain later) and they are all functions of distance (s). Here we have generalized the formalism in Ref [21] to incorporate the conditions due to structural asymmetry. Although the s-dependent functional form of M_e, M_m, and L' are complex and cannot be obtained using the Lagrangian formalism alone, we know they are fixed once s is unchanged. Because electric and magnetic dipolar interactions are always present in metamolecules, incorporating M_e and M_m terms in Eq. (1) is expected. However, after a careful inspection of their contributions by varying their signs and magnitudes, we find that M_e and M_m always yield a redshift and a blueshift. Therefore, an additional inductive term (L') must be included to incorporate all the observed phenomena. Notably, L' always reduces the total energy in Eq. (1) and thus contributes redshifts [21,22].

When the system is structurally symmetric ($\omega_1 = \omega_2$, $Q_1 = Q_2$), the last term of Eq. (1) vanishes and the couplings are dominated by the electric and the magnetic dipolar couplings. Thus it explains why previous works on structurally symmetric dimers did not observe the type III couplings. When the system is structurally asymmetric ($\omega_1 \neq \omega_2$, $Q_1 \neq Q_2$), L' may appear and it always contribute redshifts. Apparently, the contribution from L' are strong so that the type III couplings are very common in asymmetric dimers. From Fig. 1(c), we notice that the metamolecules in the type III category always exhibit parallel rods geometries in proximity to each other. In fact, our simulations have shown that the type III coupling always associates with antiparallel or parallel current flows with spatial proximity. Thus it also justifies the last term of Eq. (1).

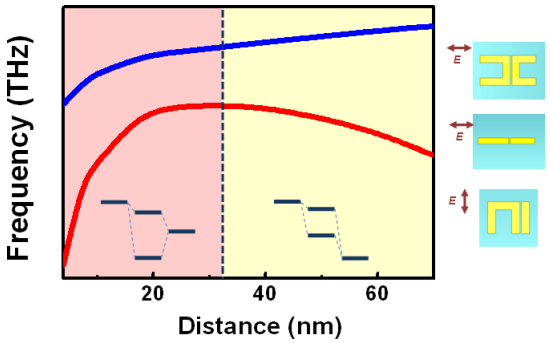

Fig. 3. Transitions from type II coupling to type III coupling as the distance between meta-atoms decreases. The figures in the right display three metamolecules that exhibit the transition. The arrows denote the polarization of the normally incident light.

The type III coupling phenomena are truly unusual, as one cannot find any analogies in mechanical systems or natural molecules. We have found that when the distance between the two meta-atoms decreases, the contribution from the last term of Eq. (1) becomes larger. As shown in Fig. 3, when the distances between meta-atoms are large, the system displays the type II coupling effect. Interestingly, when the distance decreases, the coupling displays the type III couplings. Figure 3 also shows various dimers that exhibit type II to type III transitions as the distance decreases. Unlike electric or magnetic dipolar interactions that sustains for long range distances, the deep subwavelength nature of L' indicates that it is a near field effect.

#157877 - $15.00 USD Received 8 Nov 2011; revised 28 Dec 2011; accepted 3 Jan 2012; published 24 Jan 2012

Now we show that Eq. (1) can quantitatively explain the observed phenomena. After substituting $Q_i = A_i \exp(i\omega t)$ to the Euler-Lagrangian equation, the dimers can be analyzed by solving the following determinant:

$$\begin{vmatrix} -(L_1 + L')\omega^2 + L_1\omega_1^2 & (L' + M_m)\omega^2 + M_e\omega_1\omega_2 \\ (L' + M_m)\omega^2 + M_e\omega_1\omega_2 & -(L_2 + L')\omega^2 + L_2\omega_2^2 \end{vmatrix} = 0 \quad (2)$$

Notice that M_e and M_m appear at the off-diagonal terms, thus they always yield one redshift and one blueshift with identical magnitudes. In addition, L_1 and L_2 can be approximately related to ω_1 and ω_2 by a structural-asymmetry factor ($g \equiv \omega_1 L_1/\omega_2 L_2$) for a given meta-molecule. Thus the magnitudes of the redshifts in symmetric or antisymmetric modes can be determined. Constrained by the above requirements, the only free fitting parameters are the functional forms of $M_e(s)$, $M_m(s)$ and $L'(s)$. The fitting results are shown in dashed lines in Fig. 2. It can be seen that with a few fitting parameters, the solutions of Eq. (2) can quantitatively explain all the coupling phenomena of two meta-atoms.

Now we discuss the electromagnetic origin of *L*'. The introduction of displacement current in Maxwell's equations was imposed by conservation of charge that not only unified electricity and magnetism but also predicted the existence of electromagnetic waves. In Maxwell's equations, displacement current density (J_D) is expressed as:

$$J_D = \varepsilon_r \varepsilon_0 \frac{\partial E}{\partial t} \quad (3)$$

where E is the electric field, t is time, ε_r is the relative permittivity of the filled materials, and $\varepsilon_0 = 8.854\times10^{-12}$ F/m is the vacuum permittivity. Like ordinary currents, displacement currents can also generate magnetic fields, as been verified by several experiments [23–25]. Since inductance relates electromotive forces or voltages to time-varying magnetic fields, one can anticipate that displacement currents also contribute inductance to a circuit. In addition, because the magnetic fields generated by displacement currents are proportional to the frequency, the added inductance is negligible below microwave frequencies but becomes significant at optical frequencies. Moreover, unlike ordinary currents that are carried by electric charges, displacement currents are carried by longitudinal electromagnetic waves. Thus they decay exponentially from their sources and are subwavelength in nature. When two meta-atoms move closer, ordinary surface currents originally confined in each meta-atom will start to flow from one to anther via displacement currents. The increasing displacement currents at reducing distances results in a greater contribution from the added inductance. All these features of displacement currents satisfy the properties of *L*' discussed above. Therefore, the electromagnetic origin of *L*' is Maxwell's displacement currents. We are currently investigating more novel properties arising from *L*'.

Apart from the contribution of Maxwell's displacement currents discussed above, we note that there is an alternative theory based on a plasmonic hybridization model which also claims to account for the type III coupling effect [26,27]. The plasmonic hybridization model proposes that in addition to the dipolar interactions, there are dipole-multipole interactions that give arise to the anomalous redshifts in type III couplings. Although both our model and the plasmonic hybridization model seems to agree with the observed phenomena; including signs of couplings and increasing interaction strengths at short distances, here we like to point out a particular system that the plasmonic hybridization model is not applicable.

Heterodimers made of dissimilar nanomaterials have been shown to exhibit type III coupling behaviors. In particular, optical responses of Ag-Au heterodimers have been investigated experimentally and analyzed in detail using the plasmonic hybridization model [18]. It has been found that, in contradiction to the experimentally observed type III redshifts, the plasmonic hybridization model instead predicts a type I coupling for the heterodimers. Similar effects have been found in Ag-Au heteodimers made of identical geometries, in which multipolar interactions are minimized [28]. Again, type III redshifts are observed. These phenomena are considered to be anomalous in views of the plasmonic hybridization model.

#157877 - $15.00 USD Received 8 Nov 2011; revised 28 Dec 2011; accepted 3 Jan 2012; published 24 Jan 2012

To account for the phenomena, the authors in Ref [18]. hypothesized a quasi-continuum of interband transition to be present in Au nanoparticles. Unfortunately, the proposed interband transition was not observed experimentally and thus it put the hypothesis in question. Besides, the type III redshifts still exist in exact electrodynamics calculations of Ag-Au heteodimers of identical geometries but without incorporating the interband transition [28]. We have also numerically confirmed the phenomena by simulating a heterodimer made of Al-Au nanorods of equal lengths. The Al-Au heterodimers display resonances at the infrared regime so that any contributions from interband transitions (which are usually in the ultraviolet regions), if present, can be ignored. Still, type III redshifts are observed. The inapplicability of the plasmonic hybridization model and the proposed interband transition thus call for a new model. Our model based on the added inductance contributions of Maxwell's displacement currents is not sensitive to the constituent materials and thus can explain the redshifts of the heterodimers. To determine which model is more plausible in plasmonics will require full analyses on extensive systems and is beyond the scope of the present paper. We will provide detailed discussions in our future works.

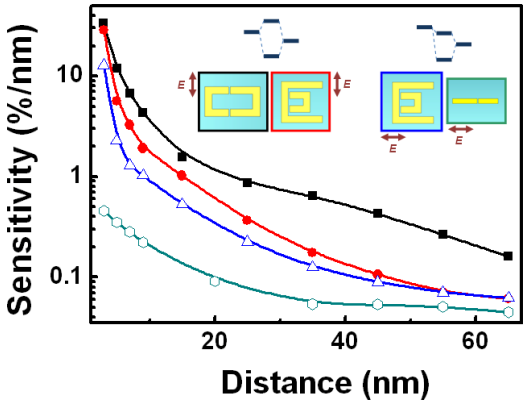

Fig. 4. Resonant frequency sensitivity vs. distance between meta-atoms for four representative metamolecules chosen from type I (black and red lines) and type III (blue and green lines) couplings (type II couplings are only observed at large distances).

From an application's point of view, what can we learn from our extensive studies? The subwavelength couplings between plasmonic elements results in concentrated electromagnetic 'hot spots' which are highly sensitive to environmental perturbations and have been employed for diverse physical, chemical, and biological sensing applications. In general, the sensitivities are correlated with the coupling strength with respect to external perturbations. As an example, we plot the highest displacement sensitivity $\Delta f/(f\Delta s)$, (where Δs = distance variation, Δf = frequency change, f = resonance frequency when $s\rightarrow\infty$) versus s from the three types of couplings in Fig. 4. The highest displacement sensitivity (35%/nm) is observed in an asymmetric split-ring resonator pair in type I. For comparison, a very high finesse (= 30000) Fabry-Perot cavity integrated with a micromechanical resonator has been reported to exhibit the highest displacement sensitivity so far [29], which corresponds to an normalized transmittance change of 25%/nm at λ = 1064 nm. For plasmonic systems, a monolayer of the asymmetric nanostructures can reach a normalized transmittance change more than 30%/nm at λ = 1550nm. Once multilayers of such asymmetric nanostructures are fabricated, more improvements can be achieved. In addition, unlike a Fabry-Perot cavity that is bulky and multi-wavelength large, the plasmonic systems are naturally deep subwavelength. Thus the structurally asymmetric plasmonic systems not only exhibit the highest displacement sensitivity among all plasmonic or non-plasmonic systems investigated so far, but also can reduce the overall size of the device by more than thousand-fold.

In summary, after extensive numerical simulations on more than twenty asymmetric plasmonic dimers, we find their coupling phenomena can be categorized into three types of

#157877 - $15.00 USD Received 8 Nov 2011; revised 28 Dec 2011; accepted 3 Jan 2012; published 24 Jan 2012

effects. The effects arise from electric and magnetic interactions that can either display positive coupling or negative coupling, and a previously unfound effect from inductance of displacement currents that always contribute frequency redshifts. Unlike the plasmonic hybridization model that fails to explain the coupling phenomena of heterdimers, our model yields consistent and quantitative agreements with the existing data. In addition, the novel effect of displacement current will open more interesting phenomena in subwavelength optics. The extraordinary coupling phenomena suggest that the interactions of metamolecules are much richer than conventional systems. It is signified in the dimers that we have identified to exhibit the highest displacement sensitivities that will pave the way for future sensing applications ranging from strain mapping, surface acoustic wave sensing, heat wave detections to integrated plasmonic-nanoelectromechanical systems.

Acknowledgments

This work was supported by the National Science Council of Taiwan (NSC98-2112-M-002-021-MY3).

#157877 - $15.00 USD Received 8 Nov 2011; revised 28 Dec 2011; accepted 3 Jan 2012; published 24 Jan 2012